Highly Sensitive, Durable and Stretchable Plastic Strain Sensors Using Sandwich Structures of PEDOT:PSS and Elastomer

Xi Fan,[†,⊥] Naixiang Wang,[†,⊥] Jinzhao Wang,[‡] Bingang Xu,[§] Feng Yan[*,†]

[†]Department of Applied Physics, The Hong Kong Polytechnic University, Hung Hom, Kowloon, Hong Kong, China

[‡]Department of Material Science and Engineering, Hubei University, Wuhan 430062, China

[§]Nanotechnology Center, Institute of Textiles and Clothing, The Hong Kong Polytechnic University, Hung Hom, Kowloon, Hong Kong, China

Abstract

Thin-film "plastic" strain sensors can be mounted closely on textile clothing or human skins comfortably to detect human activities without any harm to human body. However, it is a grand challenge to prepare highly sensitive and durable plastic strain sensors. Herein, we report a high-performance plastic strain sensor with a sandwich structure of poly(3,4-ethylenedioxythiophene):poly(styrenesulfonate) doped with poly(vinyl alcohol) (PVA−PEDOT:PSS)/highly conductive PEDOT:PSS/Polydimethylsiloxane (PDMS) elastomer. The strain sensor exhibited not only high sensitivities but also high durability at large strains owing to its robust structure integration and strong recovery ability in conductance. More importantly, our plastic strain sensors are successfully used to monitor a series of human activities including joint/muscle motions, arterial pulsation and voice vibration, and distinguish some complex and diverse bending motions, demonstrating a great potential in practical applications.

[*]Address correspondence to apafyan@polyu.edu.hk

1. Introduction

In recent years, wearable strain gauges have attracted much research interests for their broad applications on electronic skin, health monitoring, soft robotics and various medical devices.[1–6] Strain sensors are commonly composed of a stretchable conductor and two metal electrodes on its surface. The stretchable conductor plays an essential role of sensing external stimulation and can generate output resistance signals. A thin-film stretchable conductor is a typical item in a strain gauge,[3,7,8] which can be attached to a target object for high-quality monitoring. The stretchable conductor can also be integrated with flexible electronics and used as not only a strain gauge but also a flexible electrode or a channel [9,10,11]. Considering the potential applications, high-performance strain sensors should meet the following requirements:[7,8,12-17] *i*) high sensitivity (gauge factor, GF) of over 10; *ii*) high mechanical durability that enables a stable resistance response to the tensile strains (at least 20% strain for a monitor of human activities); *iii*) High conductance for low power consumption with high optical transparency; *iv*) a simple and printing/solution manufacture process; and *v*) being comfortable without allergic irritation to human skins. Although lots of efforts had been devoted to strain gauges by using metal nanowires,[7,12] metal nanoparticles,[13] carbon nanotubes,[14–16] carbonized cotton fabrics,[17] graphene,[4,6,18–20] conducting polymers,[8,21] *etc*, none of the strategies can meet the above requirements for high-performance strain gauges.

Poly(3,4-ethylenedioxythiophene):poly(styrenesulfonate) (PEDOT:PSS) has been widely employed in wearable or flexible electronic devices, such as pressure/strain sensors, flexible solar cells, light emitting diodes, and brain activity recorded transistors, due to many advantages including solution processability, high conductivity (σ) with high optical transparency (T), good bending flexibility, excellent thermal stability and biocompatibility.[22–27] However, normal PEDOT:PSS films on flexible substrates exhibited small resistance changes and low sensitivity under tensile strains.[21,25] For example, typical PEDOT:PSS films doped with dimethylsulfoxide (DMSO) prepared on polydimethylsiloxane (PDMS)[21] and PET substrates[25] were used as strain gauges with sensitivity of 5.5 and 2.5 at 20% strain, respectively. Our

group developed a plastic strain gauge using the strong acid-treated PEDOT:PSS films embedded into PDMS[8] and demonstrated sensitivity of 22 at 20% strain, which was attributed to PSS−poor fragile films and the formation of PEDOT and PDMS composites at the interfaces.[8] However, a structural collapse of the composite film occurred in cyclic stretchable tests caused a limited mechanical durability and sensible strain region. Recently, numerous efforts had been devoted to highly stretchable and durable conductors by blending elastomers such as soft polymers,[28] Zonyl FS 300 fluorosurfactant (Zonyl),[21] X-triton,[29] PDMS,[30] and ionic liquids[31,32], into PEDOT:PSS. Unfortunately, almost all the blended films are unsuitable for fabricating sensitive strain sensors because of a rather small change in resistance in loading tests, which suggests a poor value of sensitivity. For example, Wang *et al*. reported a stretchable polymer conductor of PEDOT:PSS *via* ionic liquids and acid doping.[32] Their recipe is an innovative method that endows the polymer conductors with giant conductivity and stretchability. However, the stretchable conductors failed to sense tensile strains.[32] Therefore, it is grand challenge to prepare highly sensitive, stretchable and durable plastic strain sensors.

Here, we demonstrate a novel strategy of fabricating highly sensitive and durable plastic strains sensors *via* a sandwich structure engineering. In the devices, a highly conductive PEDOT:PSS film is embedded between PDMS elastomer and a PEDOT:PSS film doped with poly(vinyl alcohol) (PVA) and Zonyl. The plastic strain sensor demonstrates high sensitivity (*e.g.*, GF≈14 at 5% strain and ≈110 at 30% strain), a stable strain sensitive region of 5%−30%, and a good durability in stretchable-releasing tests for hundreds cycles and long-time loading tests. The high sensitivity originates from a large resistance change ($\Delta R/R_o$), which is mainly induced by the formation of fine cracks in the PEDOT:PSS films by tensile stains and a subsequent connection between the cracks when the films were relaxed; whereas the high durability of the devices results from the mechanically robust integration of the sandwich structure. Therefore, high sensitivity, durability and broad strain sensitive region are simultaneously achieved in the plastic strain sensors, which satisfies the basic requirements of monitoring human daily activities such as the joint/muscle

activities. The plastic strain sensors clearly distinguish the complex bending motions at diverse bending angles *via* alternate signals, enriching the functions of plastic strain gauges.

2. Results and Discussion

2.1. Structural and Opto-electronic Property of Strain Sensors

Figure 1a and b show the schematic diagram and the picture of a stretchable conductor with a sandwich structure, respectively. The preparation process of the plastic strain sensor based on the sandwiched film is illustrated clearly in Figure S1. Notably, methanesulfonic acid (MSA) has to react fully with PEDOT:PSS and some visible smoke can be observed, which is key to obtain the high conductivity (~3100 Scm^{-1}) of PEDOT:PSS films. The high temperature acid treatment not only enables the maximum removal of insulating and viscous PSS from the matrix, but also induced very weak van der Waals forces between PEDOT:PSS and glass slides for a feasible peeling. After peeling the films from glass slides, the PVA, Zonyl FS300 and DMSO blended PEDOT:PSS films with a modest conductivity of 460 S cm^{-1} was spin-coated on the surfaces of PEDOT:PSS/PDMS. To explain the difference in conductivity of both the films, the S 2p XPS of the acid−PEDOT:PSS films and the blend PEDOT:PSS films are shown in Figure 1c. It shows that the acid treatment is more effective than the secondary solvent DMSO in removing PSS and can lead to a significant increase in the conductivity of a PEDOT:PSS film. In addition, compared with the acid−PEDOT:PSS films, the PVA−PEDOT:PSS films became more viscous and stretchable. Finally, the PVA−PEDOT:PSS/acid−PEDOT:PSS/PDMS films exhibited a transparency (T) of 75% at λ = 550 nm (see Figure 1d), indicating a potential application in transparent or semitransparent sensing devices.

2.2. Durability and Sensitivity of Strain Sensors

The mechanical repeatability of the sandwiched films is first investigated in 400-cycle stretchable-releasing tests at 10%, 20% and 30% strain, respectively, as shown in Figure 2. We found that the resistance of the films returned to the initial value ($R_o \approx$

220 Ω) in the repeated loading tests at 10% and 20% strains. Meanwhile, the sandwiched films under each strain state have no remarkable variation in resistance, demonstrating an outstanding mechanical repeatability and stability thanks to the robust structural integration of PDMS, acid−PEDOT:PSS and PVA−PEDOT:PSS. After the stretchable-relaxing test at the strain up to 30%, the sandwiched films exhibit a slight increase in resistance (from 300 to 550 Ω), which probably is resulted from the viscoelasticity of PDMS[8] and a slight abrasion of PEDOT:PSS in the harsh and repeated tests. Furthermore, long-time durability tests are conducted at the strains of 10%−30%, as shown in **Figure** 2d. Although the sandwiched films are subjected to the sustained tensile strains as long as over 120 sec, they still exhibit a stable resistance response under strains and a fast recoverability in conductance when the films are relaxed.

For comparison, the repeatability and long-time durability of the reference films with the simple structure of PEDOT:PSS/PDMS are also investigated (see Figure S2). Obviously, they show an irreversible and "abrupt" increase in resistance in 400-cycle strain/release tests. The resistance increases irreversibly up to 2400 Ω upon the repeated loading test at 20% strain, suggesting a large-domain damage of the films by the 400-cycle mechanical test. *Lee et al.* reported that an "abrupt increase" in resistance is originated from some cracks or defects generated by applied strain, which lead to physical discontinuities between regions of PEDOT:PSS films.[31] To confirm the discontinuity region that causes the increase in resistance, the long-time loading tests are carried out, as shown in Figure S2b. The reference films just afford a strain as small as 10%. With the increase of the strain up to 20%, the resistance does not recover to its initial values; whereas up to 30% stain, a large breakdown in conductance occurs, suggesting the generation of large-domain cracks and a severe discontinuity between regions of the reference films. Our results demonstrate that the sandwiched films are superior to the reference films with PEDDOT:PSS/PDMS in repeatability, long-time durability, and recoverability (at strains of ≤ 30%).

The sensitivities of the strain sensors at the stains of 5%−30% are then investigated. GF is defined as $(R/R_0)/\varepsilon$, where R/R_0 is the relative change in resistance

of the strain sensors, and ε is the applied strain. It is notable that the PVA doping content plays a significant role of determining the sensitivity of the strain gauges. With the increase of PVA doping from 2 to 10 wt %, the strain sensors show lower sensitivity. And 10 wt % PVA doping causes some large aggregation of PEDOT:PSS and a following precipitate that is difficulty to be filtered. Therefore, 2 wt % PVA doping is selected as the optimized content in this work. Figure 2e illustrates the calculated GF values at the strains of 5%−30% and the corresponding change of R/R_0, according to Figure S3. The value of GF is 14 for 5% strain, 26 for 10% strain, 70 for 20% strains, and 110 for 30% strain, respectively, demonstrating a high linearity and repeatability of GF values under the strain/release tests. In addition, the response times of the strain sensors are as short as 40 ms in quick tensile strain motions (see Figure 2f), demonstrating a fast response without obvious delays to the strain behaviors. Therefore, our sandwiched strain sensors can offer promising applications with high sensitivity, reproduction and fast response under tensile strains.

2.3 Mechanism of High Durability with Stable Resistance Response

To understand the effect of the tensile strains on the mechanically durable performance of the films, we investigate the micro-morphology of the PEDOT:PSS films using optical microscope. Figure 3a shows the morphology of the pristine sandwiched films (a) and the sandwiched films upon the 400-cycle stretchable-releasing tests at 20%, 30% and 40% strain. None of buckled structures or cracks appeared in the pristine sandwiched films. With the 400-cycle loading treatments at 20% strain, the films show the buckled structures without obvious fractures, which are perhaps induced by the relaxation of the soft PDMS elastomer[21] by the repeated loading, suggesting a reliable integration of the stretchable films. Upon the 400-cycle loading test at 30% stain, fine cracks with a density of 14/mm are generated, resulting in a slight increase in resistance of the sandwiched films.

The resistance of the sandwiched films is the summery of the initial resistance and the generated resistance caused by the geometric distortion of the films and the crack propagation. We found that there is a relationship between R and ε as follows (see

details in Figure S4):

$$R = \left[1 + 1.46(e^{536(L-L_o)} - 1)\right]R_o \quad (1)$$

Here, $\varepsilon = L - L_o$, L_o is the initial length (*i.e.*, 2.0 cm) of the films, and L is the tensile length. Figure S4b shows the relationship between R/R_o and strains. In Figure S4b, the results were obtained from the above equation and our experimental data. Obviously, the fitted curves from the equation can match well with our experimental data, demonstrating the accuracy and universality of the equation in the stain region.

When the strain increases up to 40%, serve cracks (≈35/mm) appear and cannot be connected when the films are released, leading to discontinuous conducting pathways that cause an irreversible increase in the resistance of the sandwiched films. In comparison, we also investigate the micro-morphology of the reference films of PEDOT:PSS/PDMS (see Figure 3b). It shows that the crack propagation (≈25/mm) becomes visible upon the repeated loading tests at 20% strain and cannot be connected when the films are relaxed. With the increase of the strain up to 30%, severe cracks (≈50/mm) appear in relaxed PEDOT:PSS films, leading to a large increase of the electrical resistance of the films under released states. Compared with the reference films, the robust sandwich structures enable the generated cracks to be connected (or be close each other) under the relax condition, therefore, it endowed the plastic stain sensors with high durability and stable resistance response in each cycle of strain/release. Figure 3c illustrates the schematic diagram of crack connection and separation of the sandwiched films and the reference films after loading tests.

2.4. Application of Strain Sensors

2.4.1. Wearable Strain Sensors for Sensing Human Motions. The highly sensitive and durable strain sensors have a promising application for detecting human daily activities. Here, the wearable plastic strain sensor are attached on knit swear trousers, jackets and rubber gloves. It provides a precise monitoring of numerous human motions including knee, elbow, finger and palm joints, as shown in Figure 4. Figure 4a presents the resistance response to the motions of human knees at different

frequencies (*f*). The faster the bending-releasing of the motion, the higher the *f* of the output signals. With the increase of the tensile strains of the trousers caused by knee motions, the signals become sharper step by step. It is noteworthy that the resistance of the strain gauge can be recovered when knees are relaxed fully, demonstrating a precise and stable detection to mechanical deformation. Moreover, the wearable strain sensors can monitor finger, elbow and palm activities, as shown in Figure 4b-d. In brief, *via* the output signals, the detailed joint/muscle information including frequency, strength and dynamic process can be recorded in real time and effectively.

2.4.2. Bodily Strain Sensors as Electronic Skins and Sound Signals Collectors. Thanks to the ultra-flexibility, smoothness and thinness of the plastic strain gauge, the strain gauge can be attached well on human skins to monitor the movements of the cervical artery, muscle and even to detect the human sounding information. It's found that there are no resistance changes in the films under the normal condition without bending and stretching, as shown in **Figure 5a**. When the bodily sensor is attached on the epidermis of the cervical artery, a remarkable variation in resistance to the pulses of the cervical artery is displayed. The bodily devices recorded 13 obvious peaks in a span of about 11 s, reading out 70 beats per minute of pulse rate. Therefore, the strain sensors have some potential medical applications, such as evaluating the pulmonary respiratory function and excising the wallowing function of patients. Cough is one symptom of the pulmonary respiratory diseases, while many patients with lung cancers died from asphyxiation after pulmonary surgery. Our device read out the consistent cough information which is resulted from throat expansion, as shown in Figure 5c. So it helps people to record the cough information to reduce the risk of suffocating against the diseases. Besides, the stain gauges are benefit to excising the swallowing function of the patients with dysphagia. **Figure** 5d shows the response of resistance to swallowing motions. The consistent signals are generated in 12-time swallowing motions; the frequency and strength help people to excise and evaluate their swallowing function.

In addition, a sandwiched film is stretched up to 40% strain to generate serve

crack propagation that endows the devices with the capacity of detecting very tiny and weak vibration such as human voicing. Figure 5e shows the resistance response of the strain sensor to the repeated stretchable-relaxing at 40% strain. The resistance values are very stable (≈2.5×10^7 Ω) under 21-cycle strain. The conductance of the device could be restored reversibly to the value of 850 Ω when it's relaxed, demonstrating excellent reproducibility and repeatability. Based on pre-stretched films, the strain gauges can detect sounding vibration (*i.e.*, speaking "C") when attached onto the human throats (see Supporting Information, Video 1). As seen in Figure 5f, the strain sensor can distinguish the smooth pronunciation and the disturbance of voice fluency (see the bold curves in Figure 5f) in sounding processes. The high pronunciation recognition of the devices paves a promising pathway toward the applications in human/robot pronunciation rehabilitation exercise in the future.

2.4.3. Monitoring Complex Bending Motions. Bending is one of the most common activities of human beings. Actually, it involves many complex motions (*i.e.*, bending up and down) with diverse bending angle (θ, defined in Figure 6a). To our best acknowledge, there are few strain gauges that can distinguish complex bending motions owing to the limits of sensing performance of devices. In this work, our strain sensors by the pre-stretch to 40% strain have the capability of detecting complex motions thanks to the formation of large-domain cracks in the sandwiched films. Figure 6b shows the real-time signals of R/R_o generated by human hand bending (see Supporting Information, Video 2). It should be mentioned that the strain sensor is integrated on PET substrates (thickness: ~200 μm) for a precise control of the bending angles. Actually, the motions of bending up and down induce the tension and compression of the cracks and the films, respectively, leading to a lower R under the tension model and a higher R under the compression model than R_o. Therefore, an alternate signal is generated that is the underlying mechanism of distinguishing bending motions.

Furthermore, the strain sensor can detect diverse bending angles of bending motions. Figure 6c shows the relative resistance change (R/R_o) as a function of θ in

the motion of bending down. With the decrease of θ (0→-π/4→-π/2→-π), the strain of the sandwiched film became larger, making the increase in R/R_o to 1.80, 4.25 and 4.40; and with the increase of θ (-π→-π/2→-π/4→0), the value of R/R_o recovered to 4.20, 1.50 and 0. Similar trends of resistance variation were observed in 4-cycle bending-releasing tests, demonstrating a stable and repeatable response of the plastic devices to bending. In addition, the device is capable of sensing the bending degrees of bending up, as shown in Figure 6d. The motion of bending up is accompanied by the compression of the films and the cracks, leading to decreased resistances. It distinctly detect the bending angle (θ = 0, π/6, π/3 and π/2) *via* the decreased values of R/R_o. On the basis of the above results, our plastic strain sensors are capable of distinguishing the complex bending motions with θ from -π to π/2, which riches the multifunction of plastic strain gauges.

3. Conclusion

In summary, we have fabricated a type of plastic strain sensor with high performance. The durability of the strain gauge is largely enhanced using the sandwich structure of PVA−PEDOT:PSS/acid−PEDOT:PSS/PDMS elastomer, which is contributed by the robust integration of the composites. The plastic strain sensor exhibits high sensitivity and stable resistance response both in repeated stretchable-relaxing tests and long-time loading tests due to the fine crack propagation of the sandwiched films and the connections between cracks soldered by PVA−PEDOT:PSS when the devices are relaxed. Furthermore, wearable and bodily strain sensors are integrated, which can clearly monitor a great deal of human joint/muscle activities and distinctly distinguish some complex bending motions. We believe that the new type of plastic and multifunctional strain sensors pave a promising pathway toward the bright applications due to their high sensitivity and durability.

4. Experimental Section

Preparation of sandwiched Stretchable Conductor. A common aqueous solution of PEDOT:PSS (Clevios PH 1000) was firstly filtered through a 0.45-μm syringe filter

and then was spin-coated on glass substrates (2.5 × 7.6 cm^2) to form a pristine film. Upon a thermal annealing, the dried pristine film was treated by 8.0 M methanesulfonic acid at the high temperature up to 160 ℃. Strong acid residuals were washed out by deionized water and isopropyl alcohol followed by the thermal annealing at 120 ℃. Subsequently, liquid PDMS (SYLGARD 184 SILICONE ELASTOMER from Dow Corning) was dipping on the highly conductive films (40 nm-thickness) followed by curing at 80 ℃ for 2 hours to obtain the PEDOT:PSS/PDMS films. The films were peeled from the donor glass substrates. Next, a blend film was spin-coated on the films placed on a glass slide using the aqueous solutions (Clevios PH 1000, blended with 2 wt % PVA (Molecular weight: 146K−186K), 1 vol % Zonyl FS 300 and 6 vol % DMSO). Here, 1 wt % of Zonyl was added into the solutions to enhance the wettability of the PEDOT:PSS droplets on surfaces of the underlying layers. Finally, a thermally annealing at 120 ℃ for 30 min was conducted.

Fabrication and Characteristic of Plastic Strain Sensors. (1) Measurement of sensitivity and durability. First, the sandwich films (Length: 7.0 cm; width: 2.2 cm, and height: 0.3−1.0 mm) were prepared. Two ITO-coated glass substrates were placed on a desk platform (One slide was fixed on the platform and the other could be moved in horizontal direction. The initial distance of both the substrates is about 2.0 cm). The ITO side was flipped by our stretchable films followed by a mechanical fixation using adhesive tapes. *Via* moving the other slide of ITO along horizontal direction, the resistance behavior of plastic strain sensors was recorded. Here, the operating voltage is set to 0.1 V.

(2) Application of Plastic Strain sensors. The stretchable conductor with sandwich structures was flipped and Ag wires were attached to the ends of the stretchable conductor by Ag pastes. Then, the metal electrodes were glued by liquid PDMS followed by curing at 80 ℃ for about 2 hours, which ensured a robust contact between the stretchable conductor and metal electrodes for the next monitoring.

Characterization. Transmission spectrum was measured using a Hitachi U-3010 UV−visible spectrophotometer. Film thickness was characterized using

surface profile-meter (Talysurf Series II). Electrical contacts were made by Ag pastes and indium on four points of samples. Electrical conductivity was measured using van der Pauw four-point probe method. Film morphology was investigated by optical microscopy (Nikon, Japan). Composition analysis of the films was examined by XPS (XSAM800). Response in resistance to strain was characterized using Keithley 2400 source meter.

REFERENCES

(1) Liu, Z.; Fang, S.; Moura, F.; Ding, J.; Jiang, N.; Di, J.; Zhang, M.; Lepro, X.; Galvao, D.; Haines, C.; Yuan, N.; Yin, S.; Lee, D.; Wang, R.; Wang, H. Lv, W.; Dong, C.; Zhang, R.; Chen, M.; Yin, Q.; Chong, Y.; Zhang, R.; Wang, X.; Lima, M.; Ovalle-Robles, R.; Qian, D.; Lu, H.; Baughman, R. H. Hierarchically Buckled Sheath-Core Fibers for Superelastic Electronics, Sensors, and Muscles. *Science* **2015**, *349*, 400−404.

(2) Matsuhisa, N.; Inoue, D.; Zalar, P.; Jin, H.; Matsuba, Y.; Itoh, A.; Yokota, T.; Hashizume, D.; Someya, T. Printable Elastic Conductors by in situ Formation of Silver Nanoparticles from Silver Flakes. 2017, DOI: 10.1038/nmat4904.

(3) Lee, Y. Y.; Kang, H. Y.; Gwon, S. H.; Choi, G. M.; Lim, S. M.; Sun, J. Y.; Joo, Y. C. A Strain-Insensitive Stretchable Electronic Conductor: PEDOT:PSS/Acrylamide Organogels. *Adv. Mater.* **2016**, *28*, 1636−1643.

(4) Jeong, Y. R.; Park, H.; Jin, S. W.; Hong, S. Y.; Lee, S. -S.; Ha, J. S. Highly Stretchable and Sensitive Strain Sensors Using Fragmentized Graphene Foam. Adv. Funct. Mater. 2015, 25, 4228–4236.

(5) Zhang, M.; Wang, C.; Wang, H.; Jian, M.; Hao, X.; Zhang, Y. Carbonized Cotton Fabric for High-Performance Wearable Strain Sensors. *Adv. Funct. Mater.* **2017**, *27*, 1604795.

(6) Qin, Y. Y.; Peng, Q. Y.; Ding, Y. J.; Lin, Z. S.; Wang, C. H.; Li, Y.; Xu, F.; Li, J. J.; Yuan, Y.; He, X. D.; Li, Y. B. Lightweight, Superelastic, and Mechanically Flexible Graphene/Polyimide Nanocomposite Foam for Strain Sensor Application. *ACS Nano* **2015**, *9*, 8933–8941.

(7) Amjadi, M.; Pichitpajongkit, A.; Lee, S.; Ryu, S.; Park, I. Highly Stretchable and Sensitive Strain Sensor Based on Silver Nanowire Elastomer Nanocomposite. *ACS Nano* **2014**, *8*, 5154−5163.

(8) Fan, X.; Xu, B.; Wang, N. X.; Wang, J. Z.; Liu, S. H.; Wang, H.; Yan, F. Highly Conductive Stretchable All-Plastic Electrodes Using a Novel Dipping-Embedded Transfer Method for High-Performance Wearable Sensors and Semitransparent Organic Solar Cells. *Adv. Electron. Mater.* **2017**, *3* (5) 1600471.

(9) Kim, K. S.; Zhao, Y.; Jang, H.; Lee, S. Y.; Kim, J. M.; Kim, K. S.; Ahn, J.-H.; Kim, P.; Choi, J.-Y.; Hong, B. H. Large-Scale Pattern Growth of Graphene Films for Stretchable Transparent Electrodes. *Nature* **2009**, *457* (7230), 706−710.

(10) Fan, X.; Xu, B.; Liu, S.; Cui, C.; Wang, J.; Yan, F. Transfer-printed PEDOT:PSS Electrodes Using Mild Acids for High Conductivity and Improved Stability with Application to Flexible Organic Solar Cells. *ACS Appl. Mater. Interfaces* **2016**, *8*, 14029−14036.

(11) Liao, C.; Mak, C.; Zhang, M.; Chan, H. L. W.; Yan, F. Flexible Organic Electrochemical Transistors for Highly Selective Enzyme Biosensors and Used for Saliva Testing. *Adv. Mater.* **2015**, *27*, 676−681.

(12) Park, M.; Im, J.; Shin, M.; Min, Y.; Park, J.; Cho, H.; Park, S.; Shim, M.-B.; Jeon, S.; Chung, D.-Y.; Bae, J.; Park, J.; Jeong, U.; Kim, K. Highly Stretchable Electric Circuits from a Composite Material of Silver Nanoparticles and Elastomeric Fibres. *Nat. Nanotechnol.* **2012**, *7* (12), 803−809.

(13) Luo, C. Z.; Jia, J. J.; Gong, Y. N.; Wang, Z. C.; Fu, Q.;, Pan, C. X. Highly Sensitive, Durable, and Multifunctional Sensor Inspired by a Spider. *ACS Appl. Mater. Interfaces* **2017**, *9*, 19955−19962.

(14) Yamada, T.; Hayamizu, Y.; Yamamoto, Y.; Yomogida, Y.; IzadiNajafabadi, A.; Futaba, D. N.; Hata, K. A Stretchable Carbon Nanotube Strain Sensor for Human-Motion Detection. *Nat. Nanotechnol.* **2011**, *6* (5), 296−301.

(15) Lipomi, D. J.; Vosgueritchian, M.; Tee, B. C. K.; Hellstrom, S. L.; Lee, J. A.; Fox, C. H.; Bao, Z. Skin-Like Pressure and Strain Sensors Based on Transparent Elastic Films of Carbon Nanotubes. *Nat. Nanotechnol.* **2011**, 6 (12), 788−792.

(16) Suzuki, K.; Yataka,H.; Okumiya,Y.; Sakakibara,S.; Sako, K.; Mimura, H.; Inoue, Y. Rapid-Response, Widely Stretchable Sensor of Aligned MWCNT/Elastomer Composites for Human Motion Detection. *ACS Sens.* 2016, 1, 817−825.

(17) Zhang, M.; Wang, C.; Wang, H.; Jian, M.; Hao, X.; Zhang, Y. Carbonized Cotton Fabric for High-Performance Wearable Strain Sensors. Adv. Funct. Mater. 2017, 27, 1604795.

(18) Bae, S. H.; Lee, Y.; Sharma, B. K.; Lee, H. J.; Kim, J. H.; Ahn, J. H. Graphene-Based Transparent Strain Sensor. *Carbon* **2013**, *51*, 236−242.

(19) Wu, S.; Ladani, R. B.; Zhang, J.; Ghorbani, K.; Zhang, X.; Mouritz, A. P.; Kinloch, A. J.; Wang, C. H. Strain Sensors with Adjustable Sensitivity by Tailoring the Microstructure of Graphene Aerogel/PDMS Nanocomposites. *ACS Appl. Mater. Interfaces* **2016**, *8*, 24853−24861.

(20) Chen, S.; Wei, Y.; Yuan, X.; Lin, Y.; Liu, L. A Highly Stretchable Strain Sensor Based on A Graphene/Silver Nanoparticle Synergic Conductive Network and A sandwich Structure. *J. Mater. Chem. C* **2016**, *4*, 4304.

(21) Savagatrup, S.; Chan, E.; Renteria-Garcia, S. M.; Printz, A. D.; Zaretski, A. V.; O'Connor, T. F.; Rodriquez, D.; Valle, E.; Lipomi, D. J. Plasticization of PEDOT:PSS by Common Additives for Mechanically Robust Organic Solar Cells and Wearable Sensors. *Adv. Funct. Mater.* **2015**, *25*, 427−436.

(22) Na, S. I.; Kim, S. S.; Jo, J.; Kim, D. Y. Efficient and Flexible ITO Free Organic Solar Cells Using Highly Conductive Polymer Anodes. *Adv. Mater.* **2008**, *20*, 4061−4067.

(23) Xia, Y.; Sun, K.; Ouyang, J. Solution-Processed Metallic Conducting Polymer Films as Transparent Electrode of Optoelectronic Devices. *Adv. Mater.* **2012**, *24*, 2436−2440.

(24) Kim, N.; Kee, S.; Lee, S. H.; Lee, B. H.; Kahng, Y. H.; Jo, Y.-R.; Kim, B.-J.; Lee, K. Highly Conductive PEDOT:PSS Nanofibrils Induced by Solution-Processed Crystallization. *Adv. Mater.* **2014**, *26*, 2268−2272.

(25) Tait, J. G.; Worfolk, B. J.; Maloney, S. A.; Hauger, T. C.; Elias, A. L.; Buriak, J. M.; Harris, K. D. Spray-Coated High-Conductivity PEDOT:PSS Transparent

Electrodes for Stretchable and Mechanically-Robust Organic Solar Cells. Sol. Energy Mater. Sol. Cells 2013, 110, 98−106

(26) Khodagholy, D.; Doublet, T.; Quilichini, P.; Gurfinkel, M.; Leleux, P.; Ghestem, A.; Ismailova, E.; Herve, T.; Sanaur, S.; Bernard, C.; Malliaras, G. G. In Vivo Recordings of Brain Activity Using Organic Transistors. *Nat. Commun.* **2013**, *4*, 1575.

(27) Fan, X.; Wang, J. Z.; Wang, H. B.; Liu, X.; Wang, H. Bendable ITO-free Organic Solar Cells with Highly Conductive and Flexible PEDOT:PSS Electrodes on Plastic Substrates. *ACS Appl. Mater. Interfaces* **2015**, *7*, 16287−16295.

(28) Li, P.; Sun, K.; Ouyang, J. Stretchable and Conductive Polymer Films Prepared by Solution Blending. *ACS Appl. Mater. Interfaces* **2015**, *7* (33), 18415−18423.

(29) Oh, J. Y.; Kim, S.; Baik, H.-K.; Jeong, U. Conducting Polymer Dough for Deformable Electronics. *Adv. Mater.* **2016**, *28* (22), 4455−4461.

(30) Hansen, T. S.; West, K.; Hassager, O.; Larsen, N. B. Highly Stretchable and Conductive Polymer Material Made from Poly(3,4-Ethylenedioxythiophene) and Polyurethane Elastomers. *Adv. Funct. Mater.* **2007**, *17* (16), 3069−3073.

(31) Teo, M. Y.; Kim, N.; Kee, S.; Kim, B. S.; Kim, G.; Hong, S.; Jung, S.; Lee, K. Highly Stretchable and Highly Conductive PEDOT:PSS/Ionic Liquid Composite Transparent Electrodes for Solution-Processed Stretchable Electronics. *ACS Appl. Mater. Interfaces* **2017**, *9*, 819−826

(32) Wang, Y.; Zhu, C. X.; Pfattner, R.; Yan, H. P.; Jin, L. H.; Chen, S. C.; Molina-Lopez, F.; Lissel, F.; Liu, J.; Rabiah, N. I.; Chen, Z.; Chung, J. W.; Linder, C.; Toney, M. F.; Murmann, B.; Bao, Z. N. A highly Stretchable, Transparent, and Conductive Polymer. *Sci. Adv. 2017, 3* (3), e1602076.

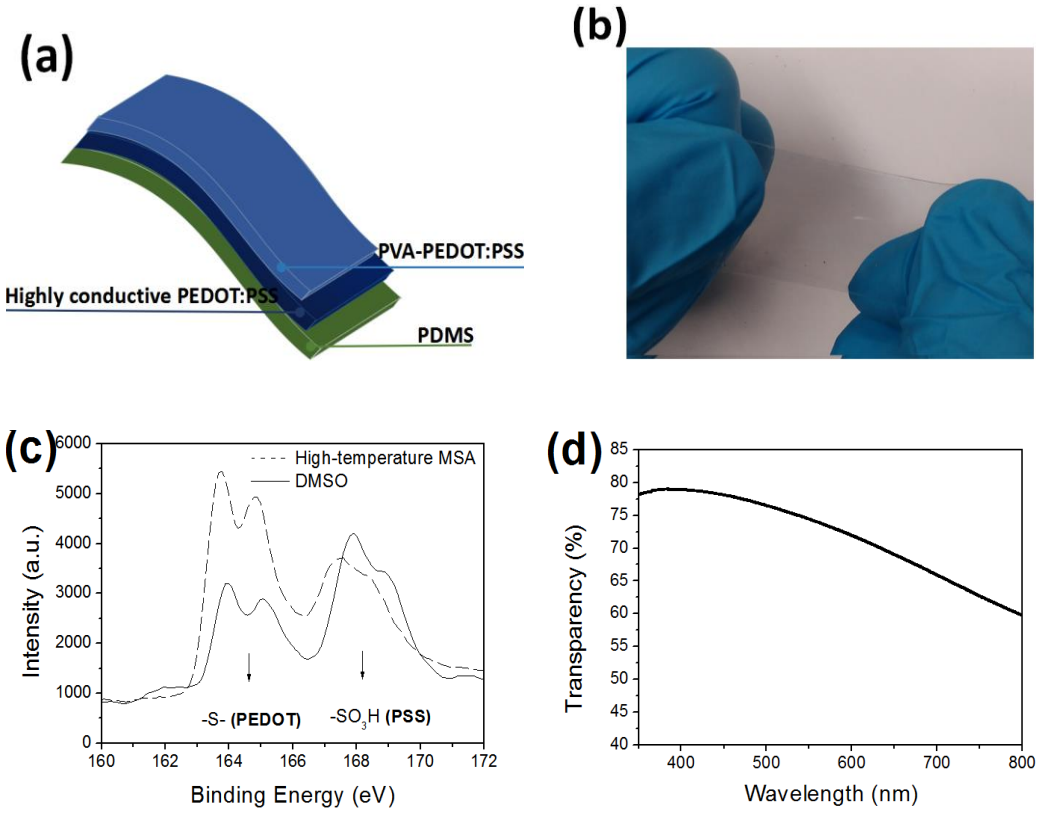

Figure 1. (a) Schematic diagram and (b) picture of the sandwiched stretchable conductor; (c) S 2p XPS of the PEDOT:PSS films by DMSO treatments and by strong acid treatments, respectively; (d) UV–visible transparency spectrum of a stretchable conductor.

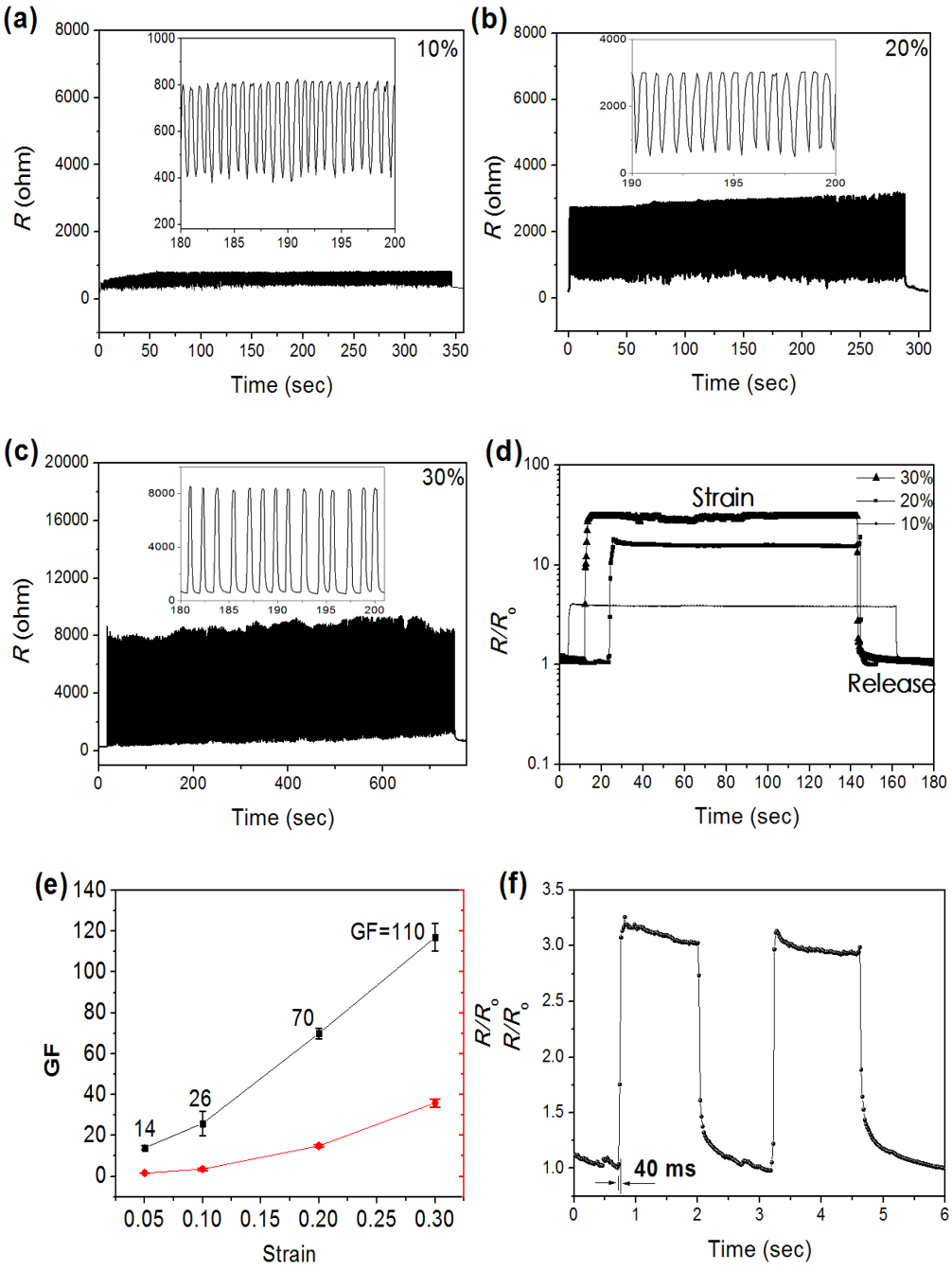

Figure 2. Resistance responses of sandwiched films in 400-cycle stretching-relaxing tests at strains of 10% (a), 20% (b) and 30% (c). (d) Resistance response in long-time loading testes. (e) Sensitivity and R/R_o as a function of strain. (f) Response time of a strain sensor in a test at about 8% strain.

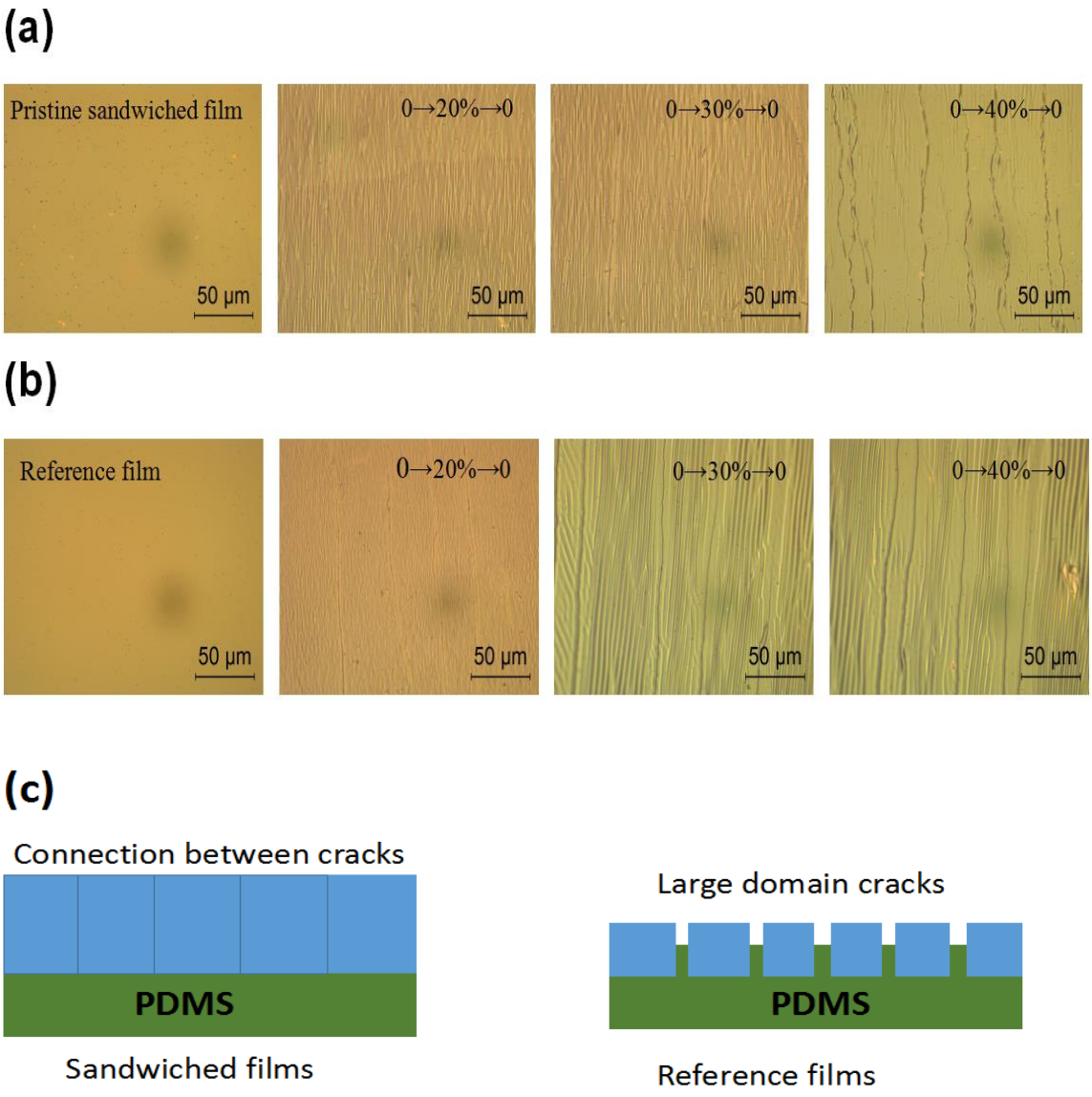

Figure 3. Micro-morphology comparison of the sandwiched films (a) and the reference films (b) with PEDOT:PSS/PDMS. (c) Schematic diagrams of crack features of sandwiched films and reference films (Blue domains represent PEDOT:PSS).

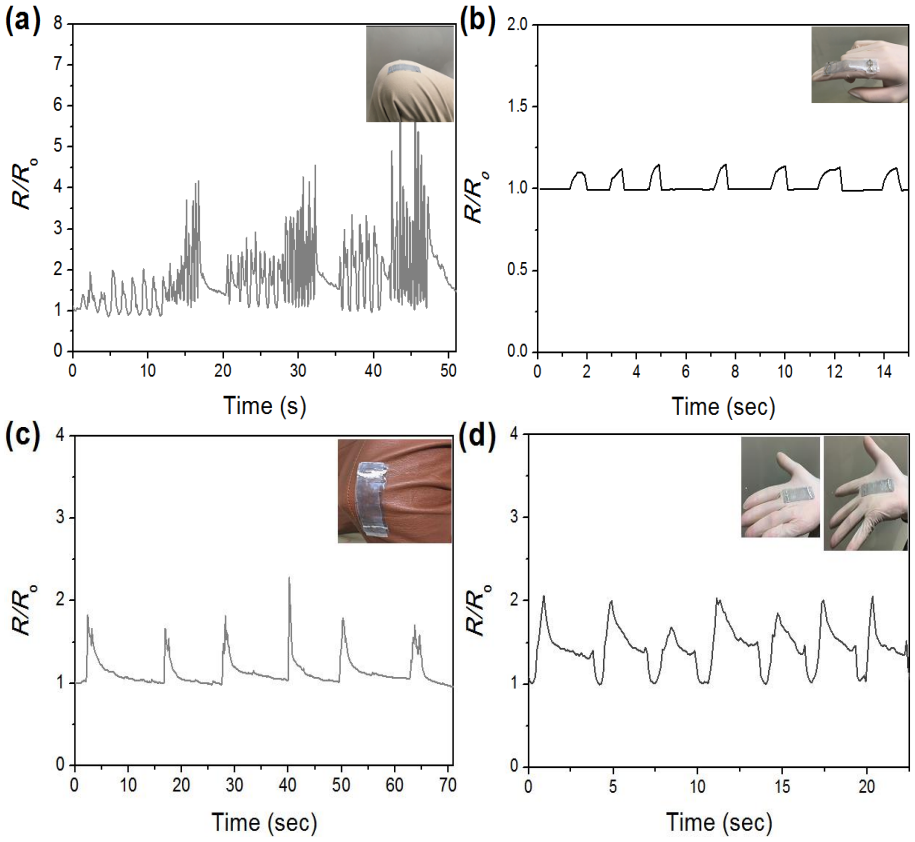

Figure 4. Real-time recording to human joint motions: (a) knee, (b) finger, (c) elbow, and (d) palm.

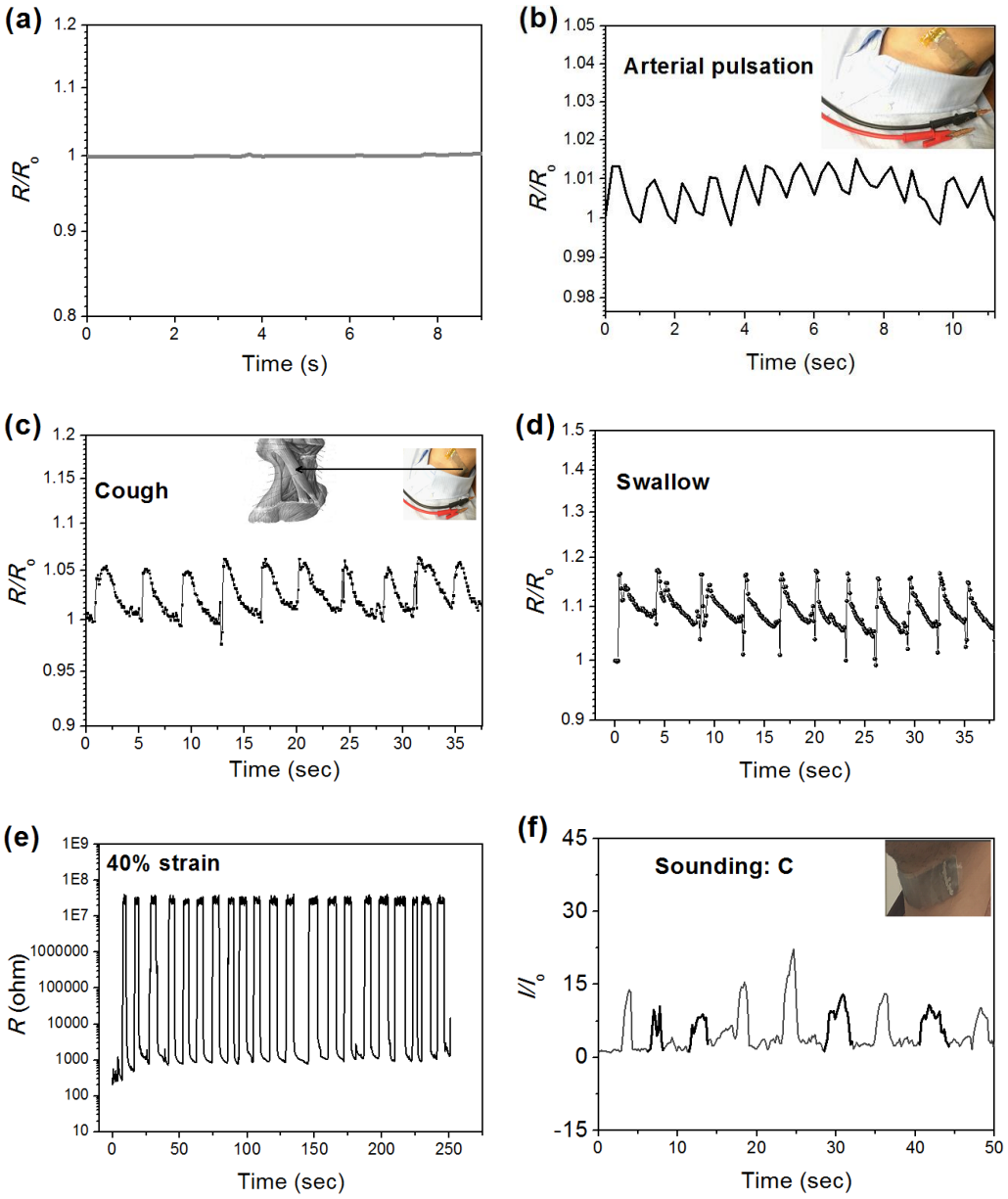

Figure 5. (a) No resistance response at normal condition. Resistance responses of the bodily sensor to "arterial pulsation" (b), "cough" (c), "swallow" (d), respectively. (e) Stable responses in resistance of the sensors in 21-cycle stretchable-relaxing tests at 40% strain. (f) A recorded signal that shows the characteristics in pronunciation: smoothness and continuity, and infinitesimal pause (Bold curves).

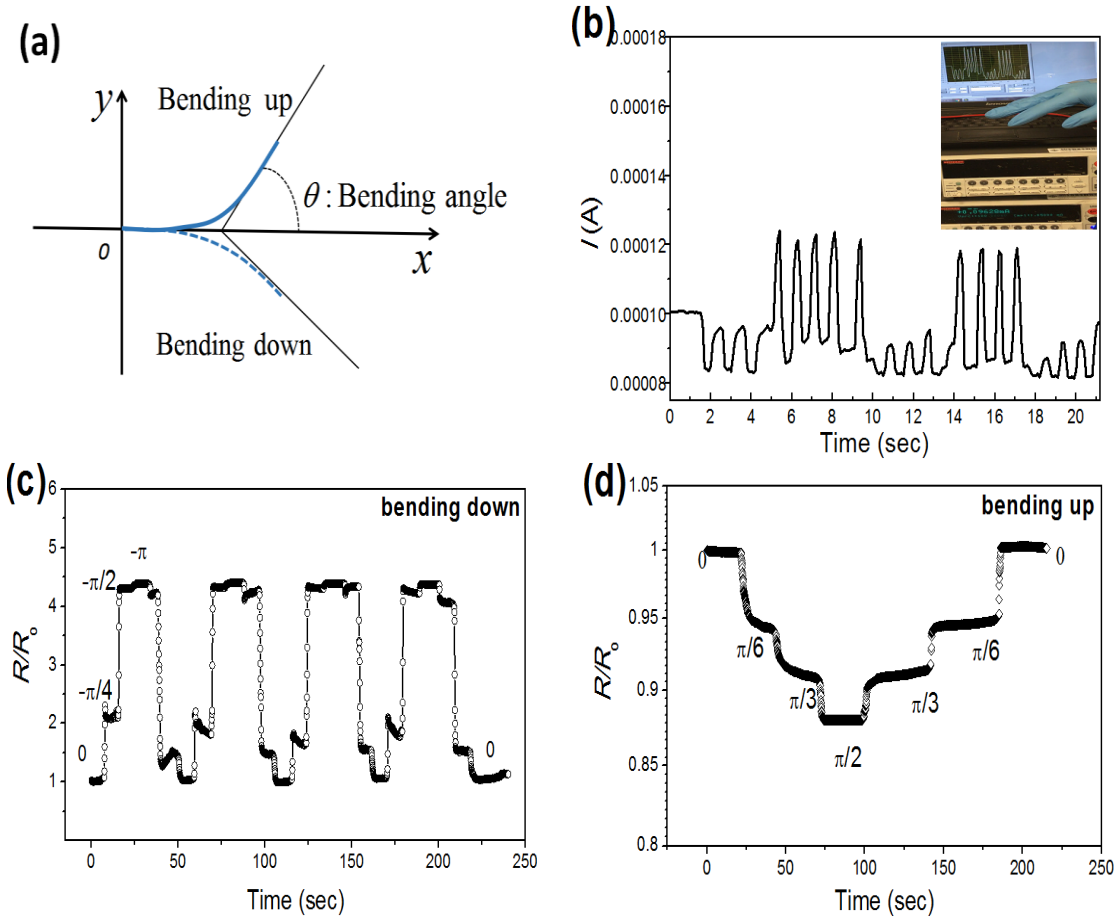

Figure 6. (a) Schematic illustration of the samples (blue) by bending up and bending down. (b) Real-time recording to the bending of the back of human hands. Inserted photography is the signals of real-time data. Response in resistance to the motions of bending down (c) and bending up (d) with different bending angles.